DOI: 10.1002/ejic.200801053

Copper(II) Oligomeric Derivatives for Deposition of Copper Thin Films

Muhammad Shahid,[a] Asif Ali Tahir,[a] Mazhar Hamid,[a] Muhammad Mazhar,*[a] Matthias Zeller,[b] Kieran C. Molloy,[c] and Allen D. Hunter[b]

Keywords: Copper / Amino alcohols / Thin films

Homobi-, -tri- and -tetranuclear copper(II) oligomeric complexes, $[Cu(dmap)(OAc)(H_2O)]_2{\cdot}H_2O$ (**1**), $[Cu_3(dmae)_3(acac)_2Cl]$ (**2**) and $[Cu(dmae)(TFA)]_4$ (**3**), have been prepared by reacting $Cu(OAc)_2{\cdot}H_2O$ with dmapH, $[Cu(dmae)Cl]_4$ with Na(acac) and $Cu(dmae)_2$ with $Cu(TFA)_2$ [dmae = (*N*,*N*-dimethylamino)ethanolate, dmap = (*N*,*N*-dimethylamino)propanolate, TFA = trifluoroacetate, and acac = 2,4-pentanedionate], respectively and characterized by melting point, elemental analysis, FT-IR and single-crystal X-ray diffraction. The crystal analysis shows that bi- (**1**) and trinuclear (**2**) complexes crystallize in the triclinic, while the tetranuclear complex **3** belongs to the monoclinic crystal system. TGA and AACVD experiments prove that the complexes undergo facile thermal decomposition in the temperature range 300–460 °C to deposit thin films of pure copper metal. The SEM and XRD analyses of the thin films suggest the formation of Cu crystallites with grain sizes of 100–340 nm (for **1**), 75.4–90.8 nm (for **2** and **3**).

Introduction

In the last two decades, evolutionary studies have been carried out for the synthesis and characterization of polymetallic clusters and cages[1,2] as these compounds have proved to be a solidly built stimulus for developments in several fields of magnetochemistry,[3,4] solid-state physics[5–7] and materials science.

Almost all transition metals throughout the periodic table form compounds utilizing different kinds of bridging organic and inorganic ligands.[1,8,9] The involvement of carboxylato, oxo and alkoxo bridges provide interesting exchange coupling in most of the cases. In this sense, alkoxo-aliphatic ligands or simple amino alcohol ligands can be expected to improve the coupling between two or more metal centers, forming homo or heteronuclear complexes.[10,11]

Current interest is in the investigation of stable and soluble homonuclear molecular complexes for their possible applications in MOCVD and chemical sol-gel processes.[12] Our particular focus is in those systems involving copper atoms since this element is the major component in high temperature super-conductors[13] and metallic copper CVD components. The copper metal has the advantage of low resistivity, enhanced electromigration resistance and improved resistance to the formation of stress-induced voids due to a higher melting point over other conducting metals such as especially aluminum. In thin-film technology, copper metal has tremendous potential for fabricating of metal interconnections, filling contacts and vial holes for designing ultra-large-scale integrated (ULSI) circuits.[14] Furthermore, copper metal provides enhanced device performance related to reduced cross talk, improved operational speed and RC delay etc.[15]

The successful contribution of precursors towards the required material and desired device fabrication is mainly dependent upon the precursor properties. They must have solubility in common organic solvents, volatility and stability to ambient environment and a large thermal window between volatilization and decomposition. Previously used classes of Cu(II) complexes utilized ligands such as fluorinated[16] and simple β-diketonates and β-ketoiminates.[17] These β-diketonate precursors are stable enough to be cleanly decomposed to metallic copper at low temperature. However, in the absence of an external reducing agent, these reagents often undergo unwanted thermal degradation leaving carbon and other contaminants (CuO) on the thin film. Another group of Cu^{II} complexes, aminoalkoxides, have been successfully employed for the synthesis of high *T*c superconductor $YBa_2Cu_3O_{7-x}$ particles[18] and metallic thin films.[19–21] Afterwards many investigators proceeded to the synthesis of simple and fluorinated amino-alcoholic complexes of copper and studied the pyrolysis mechanism in the presence of N_2 to metallic copper.[22] Another regime relying on the utilization of heteroleptic copper complexes is based on (hfac)CuL complexes (hfac = hexafluoroacetylacetonate, L = phosphane, alkyne, or olefin) for deposi-

[a] Department of Chemistry, Quaid-I-Azam University, Islamabad 45320, Pakistan
Fax: +92-51-90642241
E-mail: mazhar42pk@yahoo.com
[b] STaRBURSTT-Cyberdiffraction Consortium at YSU and Department of Chemistry, Youngstown State University, 1 University Plaza, Youngstown, Ohio 44555-3663, USA
[c] Department of Chemistry, University of Bath, Claverton Down, Bath, BA2 7AY UK

tion of metallic copper,[23] the most studied and commercialized compound being (hfac)Cu(VTMS) [where VTMS is vinyltrimethylsilane], that drew the attention towards copper aminoalkoxides.[24] However, (hfac)Cu(VTMS) can only be used together with a stabilizer and requires low temperature storage as it starts to decompose above 60 °C.[25]

Results and Discussion

Heterocatenation in copper complexes in which copper metal is encapsulated by different chelating ligands to give homometallic multinuclear molecular blocks with simple geometric configurations is common. Such molecular species can be easily prepared by simple dissolving of Cu^{II} alkoxides, β-diketonates or carboxylates with suitable ligands that have atoms which can bridge two or more copper atoms in an appropriate solvent such as toluene or THF. Using this general strategy, oligomeric complexes **1**, **2** and **3** were prepared (Scheme 1) and successively characterized by melting point, elemental analysis, FT-IR spectroscopy, and single-crystal X-ray diffraction.

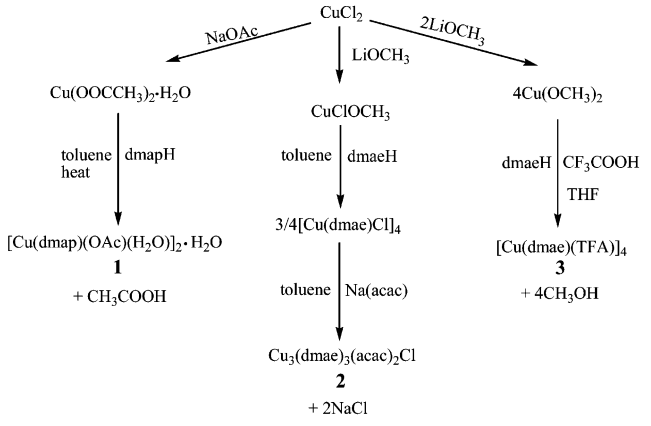

Scheme 1. Synthetic methodology adapted for the preparation of copper cages **1**, **2** and **3**.

Infrared absorption frequencies were used to establish structural similarities and differences between the three complexes. Complex **1** is characterized by a broad absorption ν_{OH} band at 3428 cm^{-1} originating from solvate water molecules present in the crystals of the complex. Similar features are absent in the spectra of the anhydrous complexes **2** and **3**. Other characteristic bands are asymmetric and symmetric CO_2 vibrations caused by the monodentate acetate (for **1**) and TFA (for **3**) registered at 1668 and 1414 cm^{-1} and at 1692 and 1593 cm^{-1}, respectively. A difference of $\nu_{asy}CO_2$ and $\nu_{sy}CO_2$ vibrations for **3** suggests the carboxylate unit of the TFA ligand to be bridging. In complex **2**, the bands at 1579 and 1551 cm^{-1} are assigned to $\nu_{C=C}$ and $\nu_{C=O}$ vibrations. The spectrum of **3** is also characterized by two strong C–F and C–O absorption bands at 1202 and 1135 cm^{-1} corresponding to TFA ligands. The absorption bands in the range of 513–525 cm^{-1} in all three complexes fall in the region reported for Cu–O bond vibrations,[26] while the absorption bands in the frequency range 432–465 cm^{-1} are due to the ν_{Cu-N} vibrations.[27]

Crystal structure data and structure refinement details for compounds **1**, **2**, and **3** are given in Table 2. The molecular structure of complex **1** is shown in Figure 1 and selected bond lengths and angles are listed in Table 1. Complex **1** is bimetallic in nature and the molecule is located on a crystallographic inversion center. The two equivalent copper atoms have a slightly distorted square pyramidal geometry with a CuO_4N coordination sphere. The dmap ligand is chelating each one of the copper atoms and its deprotonated oxygen atom bridges between the two copper centers. The forth axial position at the copper atom is occupied by an oxygen atom of a monodentate acetate ligand and the apical ligand is a coordinated water molecule. The square pyramidal geometry of the metal centers is slightly distorted with angles at the copper ion between 86.92(5) and 93.10(5)°. The metal–metal separation between the two copper centers is 3.033(5) Å. Individual molecules are connected with each other via a series of hydrogen bonds between the coordinated water molecule, another interstitial water molecule and the uncoordinated oxygen atom of the acetate ligand. Four water molecules form a clinched hydrogen bonded square with two acetate O atoms of neighboring molecules being connected to opposing interstitial water molecules of the square. Neighboring molecules are thus connected to form infinite chains parallel to the *a* axis of the unit cell.

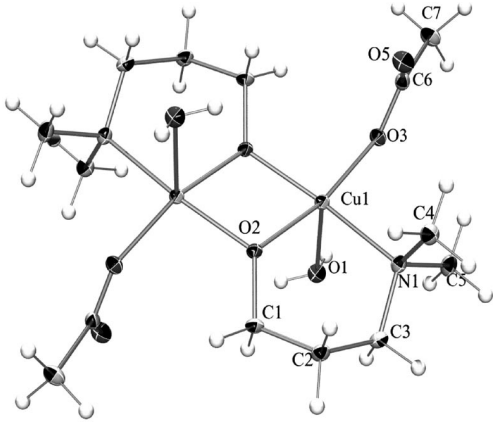

Figure 1. ORTEP drawing showing the molecular structure of $[Cu(dmap)(OAc)(H_2O)]_2 \cdot H_2O$ (**1**). Thermal ellipsoids are drawn at the 40% probably level. Interstitial water molecules are omitted for clarity.

An ORTEP diagram showing the molecular structure of **2** is given in Figure 2 and selected bond lengths and bond angles are listed in Table 1. In the solid-state structure, three Cu atoms are bridged by dmae oxygen atoms of coordinating ligands. In the core unit of the complex (Figure 2, b), two of three Cu atoms are bridged through three oxygen atoms each, while one metal center has direct interaction

Table 1. Selected bond lengths [Å] and angles [°] for complex **1**, **2** and **3**.

	1		
Cu(1)–O(2)	1.9282(11)	Cu(1)–O(1)	2.3761(12)
Cu(1)–N(1)	2.0582(13)	Cu(1)–Cu(1)#1	3.0334(5)
O(2)–Cu(1)–O(3)	167.79(5)	O(3)–Cu(1)–N(1)	93.59(5)
O(2)#1–Cu(1)–O(3)	92.98(5)	O(3)–Cu(1)–O(1)	93.10(5)
O(2A)#1–Cu(1)–N(1)	172.58(5)	N(1)–Cu(1)–O(1)	86.92(5)
	2		
Cu(1)–Cl(1)	2.2245(6)	Cu(2)–O(3)	2.0202(16)
Cu(1)–Cu(2)	2.961(16)	Cu(2)–Cu(3)	2.830(16)
Cu(1)–Cu(3)	2.958(17)	Cu(3)–O(3)	1.9695(16)
Cu(1)–O(6)	2.695(17)	Cu(3)–O(1)	2.3446(16)
O(2)–Cu(1)–O(1)	76.96(6)	O(1)–Cu(2)–N(2)	153.82(7)
O(1)–Cu(1)–Cl(1)	174.91(5)	O(2)–Cu(2)–O(1)	70.65(6)
O(2)–Cu(1)–Cl(1)	99.32(5)	O(2)–Cu(3)–N(3)	165.35(7)
O(3)–Cu(2)–O(4)	172.42(7)	O(2)–Cu(3)–O(1)	65.95(6)
	3		
Cu(1)–O(11)	1.949(3)	Cu(3)–O(1)	2.814(3)
Cu(2)–O(5)	1.963(3)	Cu(3)–O(7)	1.955(2)
Cu(3)–O(3)	1.935(2)	Cu(3)–N(3)	2.056(3)
Cu(3)–O(2)	1.947(2)	Cu(4)–O(9)	1.951(3)
O(1)–Cu(1)–O(11)	169.91(11)	O(2)–Cu(3)–O(7)	96.06(10)
O(4)–Cu(1)–N(1)	171.77(12)	O(3)–Cu(3)–N(3)	85.71(11)
O(2)–Cu(2)–O(5)	173.42(12)	O(2)–Cu(3)–N(3)	174.01(11)
O(3)–Cu(3)–O(7)	167.96(11)	O(3)–Cu(4)–O(9)	94.96(11)

with four oxygen atoms. The triangular plane of the three copper atoms is capped above and below by triply bridged oxygen atoms of two dmae ligands. The distances between these three metal centers span a considerable range: Cu(l)–Cu(2) 2.961(16), Cu(1)–Cu(3) 2.958(17) and Cu(2)–Cu(3) 2.830(16) Å. The relatively shorter Cu(1)–Cu(3) distance as compared with the Cu(l)–Cu(2) distance is probably caused by an asymmetric coordination of the two acac ligands located on both sides of the molecule towards the Cu atom Cu(1) of the Cu–Cl unit. Both acac ligands coordinate in a chelating fashion with each one copper atom [Cu(3) and Cu(2), respectively]. However, only one of the acac ligands form an additional bond towards Cu(1) via oxygen atom O(6). Towards the other side of the Cu–Cl unit the equivalent oxygen atom O(4) of the other acac ligand does not bind to the copper atom. Cu(1) is thus dragged significantly away from the median plane of the molecule towards O(6). This asymmetry is also evident by the dihedral angles between the O(1)–Cu–O(2) planes which are 47.17° between O(1)–Cu(1)–O(2) and O(1)–Cu(2)–O(2), but 57.95° between O(1)–Cu(1)–O(2) and O(1)–Cu(3)–O(2).

As expected, all the three dmae ligands are bonded to Cu atoms in a chelating/bridging fashion. As mentioned above, the deprotonated oxygen atoms of two of the dmae ligands are coordinated to three copper atoms each in a similar fashion as found in $[Cu(dmae)Cl]_4$.[26] The O atom of the third dmae molecule is bonded to two Cu centers: Cu(2)–O(3) 2.0202(16), Cu(3)–O(3) 1.9695(16) Å which is in good agreement with similar compounds.[28]

Selected bond lengths and angles for **3** are listed in Table 1, its molecular structure is delineated in Figure 3. In case of complex **3**, the core of the neutral molecule is an

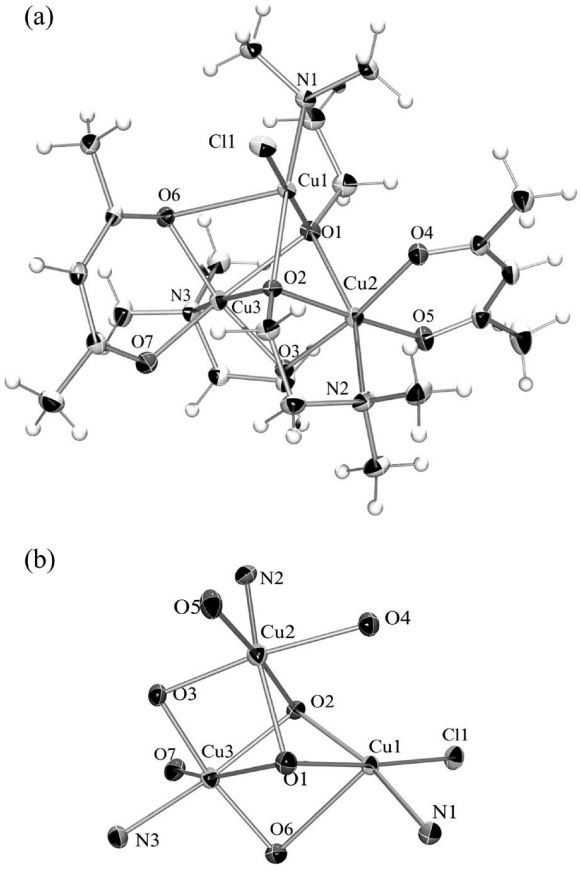

Figure 2. (a) ORTEP drawing showing the molecular structure of $Cu_3(dmae)_3(acac)_2Cl$ (**2**); thermal ellipsoids are drawn at the 30% probability level. (b) Core unit of the complex with the coordination arrangement around the Cu^{II} centers.

irregular open face Cu_4O_4 cubane (Figure 3, b). In the cubane, the copper and triply bridging oxygen atoms of dmae are arranged at alternate vertices of the cube. Cu–O bond lengths within the Cu_4O_4 cubane do vary, and Cu(3) and O(1) are separated by a distance larger than a usual Cu–O bond (2.814 Å), thus leaving the cubane motif incomplete.

Ignoring this extended Cu(3)–O(1) bond, all cooper atoms have a distorted octahedral geometry and each is six-coordinate and bonded to three alkoxy groups of the cubane, an amine and two carboxylate oxygen donors from two different trifluoroacetate ions. The trifluoroacetates bridge between two copper atoms diagonally cross a face of the cubane, while each aminoethanol unit lies along an edge of the Cu_4O_4 structure. All the copper centers show the expected distortion typical for Cu^{II} complexes that are forced into an octahedral or pseudooctahedral environment. The direction of the distortion lies along one of the carboxylate–Cu–alkoxy axes; each alkoxy group therefore has one Cu–O bond which is significantly longer than the other two. This is most pronounced for Cu(3) for which, as mentioned above, the Cu(3)–O(1) is reduced to a weak interaction and Cu(3) thus has actually a five-coordinate CuO_4N coordination sphere with a square pyramidal geometry.

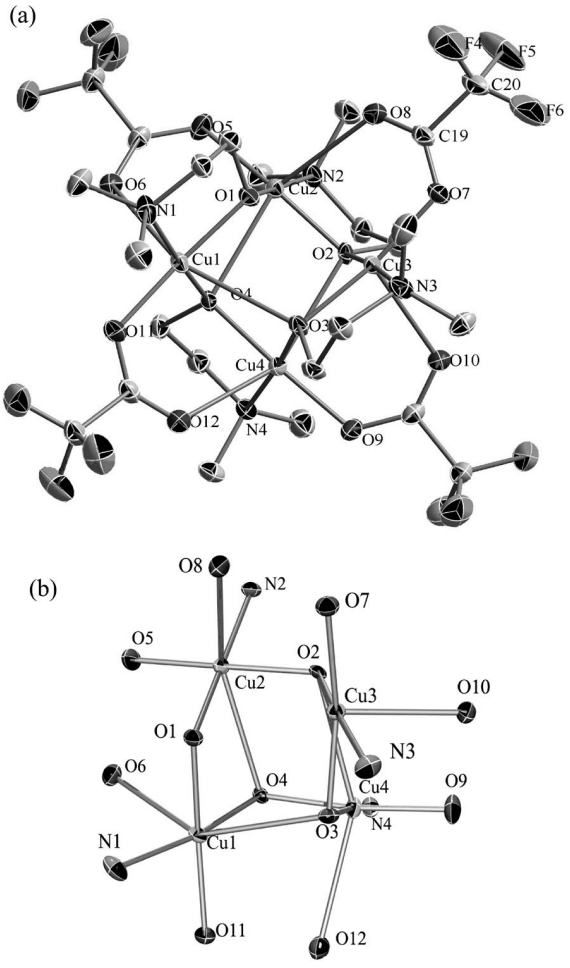

Figure 3. (a) ORTEP drawing showing the molecular structure of $[Cu(TFA)(dmae)]_4$ (**3**); thermal ellipsoids are at the 40% probability level. All hydrogen atoms are omitted for clarity. (b) Core unit of the complex with the coordination arrangement around the Cu^{II} centers; atoms are drawn at 30% probability level.

All three complexes show the tendency of Cu^{II} to avoid a symmetrical octahedral or pseudooctahedral environment wherever possible, even if the coordination environment of the ligands dictates such an arrangement. In the case of dimeric **1** all the ligands could be arranged in an essentially 2D planar way around the Cu atoms and the Cu^{II} centers can assume their preferred square pyramidal geometry with the apical positions being occupied by the water molecules. No significant distortion of Cu–O bond lengths is thus observed for the dimeric complex. In complexes **2** and **3**, however, with a larger number of coordinating ligand donor atoms vs. copper centers, this is not possible any more and the metal centers are forced into a pseudooctahedral environment, followed by distortion of the Cu–O bonds as described above. For both compounds **2** and **3** one can, however, assume that the distortions observed are fluxional once packing effects in the solid state are removed, and both in solution and in the gas phase the complexes can be assumed to easily flip back and forth between a series of energetically very similar metal ligand arrangements.

Pyrolysis Studies, Thin Film Deposition and Characterization

The TG curve of complex **1** (Figure 4, a) performed under an inert atmosphere of flowing nitrogen shows four major stages of weight loss upon heating. The first, occurring at 50–121 °C, is associated with a 14.99% weight loss which agrees well with both the coordinated and interstitial water molecules being expelled (13.82%). Immediately after the complex itself starts breaking down and in the second step between 121–167 °C a weight loss of 7.41% is observed. The third step, which starts at 167 °C and is completed at 264 °C, is associated with the largest weight loss of 47.53%, which is directly followed by the last stage ranging from 264 °C to about 450 °C, resulting in a residue amounting to 24.73% of the initial weight. This residual weight (24.73%) is very close to the expected amount (24.37%) for Cu metal.

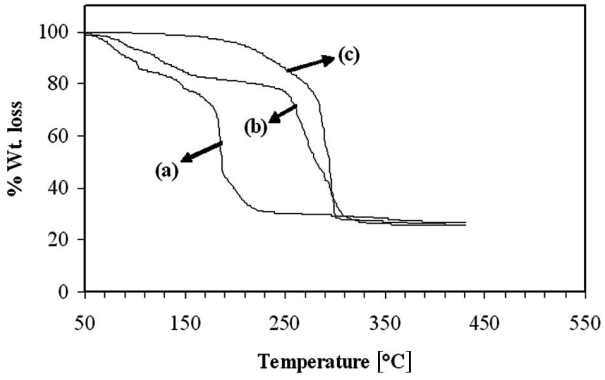

Figure 4. Thermogravimetric plot showing loss in weight with increase in temperature for complexes **1** (a), **2** (b) and **3** (c).

The TGA curve of complex **2** (Figure 4, b) shows five stages of weight loss. The decomposition starts at 71 °C and is completed at 350 °C. In the first three consecutive steps between 71 °C to 255 °C, a weight loss of 21.55% occurs. The forth one starts at 255 °C and is completed at 276 °C with a weight loss of 39.52%, which is directly followed by the last stage ranging from 276 °C to about 350 °C, resulting in a residue amounting to 25.99% of the initial weight. The residual mass of 25.99% is slightly less than expected for Cu metal (27.68%). The TGA pattern of **3** (Figure 4, c) shows a one step weight loss starting at about 175 °C and decomposition ends at about 300 °C to leave a residue of 27.76% of the initial mass. This is slightly higher than 26.31%, calculated for a complete conversion to Cu metal. The residual weight remains the same from 300 °C to 500 °C, which indicates the conversion to copper metal for all three compounds. The thermogravimetric analysis of precursors **1**, **2** and **3** performed under an inert atmosphere indicates that all three precursors have a low enough decomposition temperatures to be suitable for the deposition of copper metal thin films. Best suited, however, is complex **3** as it lacks the multi-step decomposition patterns of precursors **1** and **2**.

Thin films of the copper metal were prepared as described in the experimental section and were studied and characterized by SEM, EDX and powder XRD. The films prepared from all three precursors exhibit a good adhesion to the substrate as verified by the "scotch tape test" and are stable toward air and moisture. They reflect light in multishaded colors depending upon the thickness of the deposited films and the denser parts of the films shine in the red metallic luster characteristic for copper. Energy dispersive X-ray analysis proves the presence of metallic copper in the case of films deposited using argon. EDX analysis also proves the clean decomposition of the complexes without incorporation of impurities either from the organic parts of the complexes or the carrier gas, and ensures the formation of pure copper metal thin films.

SEM images of copper metal thin films deposited from complexes **1**, **2** and **3** (Figure 5) show compact and smooth film morphologies with homogenously dispersed particles. Individual grains are well defined with clear boundaries. The packing density of the microstructure and the grain sizes apparently seem to be affected by variation of the deposition temperature. In the case of **1**, where a temperature of 450 °C was employed, a compact dense morphology was obtained. At the lower temperatures of 350 and 300 °C used for **2** and **3** the roughness of film is more pronounced. The deposition was done at the minimum temperature for each complex at which Cu metal could be deposited as found by the TGA analysis. The SEM also shows the growth of few particles in somewhat elongated shape, (Figure 5, b) which are more clearly indicated by the SEM micrograph of thin film deposited from precursor **3** (Figure 5, c).

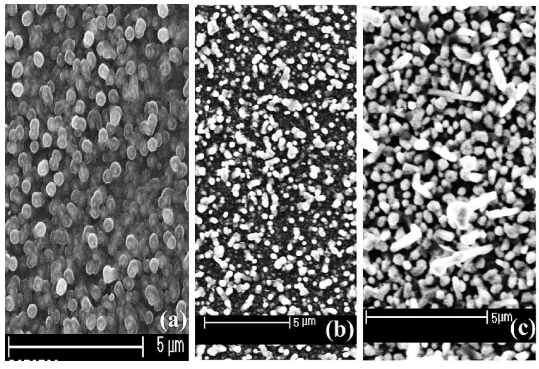

Figure 5. SEM micrographs of thin films deposited on a glass substrate (a) for complex **1**, (b) for **2** and (c) for **3** using argon as the carrier gas.

Powder X-ray diffraction patterns of the thin films deposited under argon from precursors **1**, **2** and **3** are shown in Figure 6. The *hkl* values (111), (200) and (220), 2θ values 43.43°, 50.60°, 74.19° and the corresponding d-spacings, 2.087, 1.806 and 1.273 Å, respectively, were used to determine the lattice parameter which refined to 3.616 Å assuming a cubic cell. The position and the integral width of the X-ray diffraction peaks indicate a face centred cubic lattice and the relative peak intensities and the positions of the diffraction peaks of the pattern match closely those of the ICDD data for Cu [03-065-9026].[29] The particle sizes as calculated by the Scherrer equation are 200, 75.4 and 90.8 nm for **1**, **2** and **3**, respectively and are comparable to the values determined by SEM.

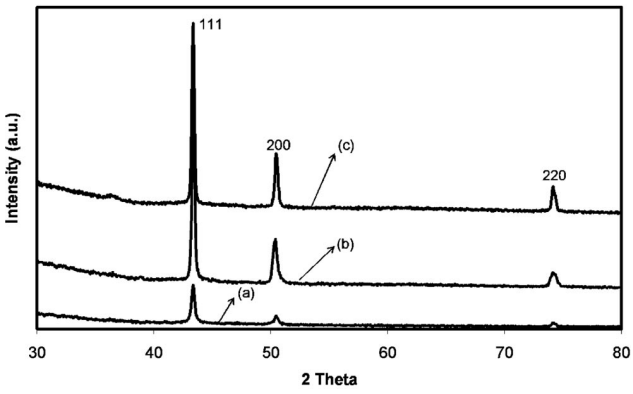

Figure 6. The XRD patterns of thin films deposited on glass substrate; (a) for complex **1**, (b) for **2** and (c) for **3** using argon as carrier gas.

Conclusions

Three oligomeric copper complexes **1**, **2** and **3** have been successfully designed, synthesized and characterized by melting point, elemental analysis, FT-IR, TG and single crystal analysis. These precursors have sufficient solubility in non-polar solvents such as toluene and THF, and the required stability and volatility for the deposition of good quality copper thin films on a non-crystalline substrate by aerosol-assisted chemical vapor deposition. The deposited thin films are characterized by SEM, EDX and XRD for their morphology and crystallinity for applications in high performance miniaturized devices.

Experimental Section

General: All manipulations were carried out under an inert atmosphere (dry argon) using Schlenk tube and glovebox techniques. Solvents were rigorously dried with sodium benzophenoate. *N*,*N*-dimethylaminoethanol (dmaeH) and *N*,*N*-dimethylaminopropanol (dmapH) were purchased from Aldrich and dried by refluxing over K_2CO_3 for 10 h and distilled immediately before use. All other reagents were purchased from Fluka. $[Cu(dmae)Cl]_4$ was synthesized using a literature procedure.[26] Melting points were determined in a capillary tube using an electrothermal melting point apparatus, model MP.D Mitamura Riken Kogyo (Japan) and are uncorrected. Elemental analyses were performed using a CHN analyzer LECO model CHNS-932. FT-IR spectra were recorded from KBr discs with a Spectrum-1000 spectrometer of Perkin–Elmer. TGA measurements were carried out using a Seiko SSC/S200 thermal analyzer at a heating rate of 10 °C/min under N_2 flow. Powder XRD studies were carried out by means of a Bruker AXS D8 diffractometer using monochromatic Cu-K_α radiation. The morphology of films was determined by scanning electron microscopy using a FEG-SEM Philips XL30. Samples were carbon-coated before observation and EDAX-DX_4 was used to calculate the composition of films.

Single Crystal X-ray Crystallography: Single crystal diffraction data of complexes **1** and **3** were collected on a Bruker AXS SMART APEX CCD diffractometer at 100(2) K using monochromatic Mo-K_α radiation with omega scan technique. The unit cells were determined using SAINT+ and the data were corrected for absorption using SADABS in SAINT+.[30] The structures were solved by direct methods and refined by full-matrix least-squares against F^2 with all reflections using SHELXTL.[31] Refinement of extinction coefficients was found to be insignificant. All non-hydrogen atoms were refined anisotropically. Water hydrogen atoms in **1** were located in the difference density Fourier map and have been refined with an isotropic displacement parameter 1.5 times that of the adjacent oxygen atom. The O–H distances were restrained to be 0.84(2) Å. All other hydrogen atoms were placed in calculated positions and were refined with an isotropic displacement parameter 1.5 (methyl) or 1.2 times (all others) that of the adjacent carbon atom.

In case of **3**, the carbon atoms of two of the dmae ligands are disordered over each two positions with occupancy ratios of 0.587(5) to 0.413(5) and 0.685(6) to 0.315(6). Equivalent bonds within the disordered moieties were set to be the same within a standard deviation of 0.02 Å and equivalent atoms were set to have identical anisotropic displacement parameters. All other hydrogen atoms were placed in calculated positions and were refined with an isotropic displacement parameter 1.5 (methyl) or 1.2 times (all others) that of the adjacent carbon atom.

Diffraction data of complex **2** were collected at 150(2) K using a Nonius Kappa image plate diffractometer using monochromatic Mo-K_α radiation. The unit cell was determined, the reflections were integrated and scaled with the HKL Denzo-Scale pack suite of programs[32] and the data were corrected for absorption using Sortav.[33] The structure of **2** was solved by direct method using SIR97[34] and refined by full-matrix least-squares on F^2 using SHELXL97.[35] All non-hydrogen atoms were refined anisotropically. Table 2 summarizes the crystal data and refinement details for all the three complexes.

Syntheses and Characterization of Complexes 1–3

Synthesis of [Cu(dmap)(OAc)(H$_2$O)]$_2$·H$_2$O (1): 0.24 g (2.33 mmol) of dmapH was added dropwise from a syringe under inert atmosphere of argon gas to a suspension of 0.50 g (2.50 mmol) of copper(II) acetate monohydrate [Cu(OAc)$_2$·H$_2$O] in toluene (20 mL). The mixture was stirred for 2 h at room temperature and further heated to 40 °C in an oil bath for another 2 h. The excess of Cu(OAc)$_2$·H$_2$O was removed by filtration through a cannula. The filtrate was evaporated to dryness under vacuum and the solid was redissolved in 5 mL of toluene to give blue crystals after 5 d by slow evaporation at room temperature; yield 85%, m.p. 55 °C. The analysis of the resulting product resembled that for [Cu(dmap)(OAc)(H$_2$O)]$_2$·H$_2$O, as determined by X-ray crystallography. $C_{14}H_{38}Cu_2N_2O_{10}$ (521.54): calcd. C 32.24, H 7.34, N 5.37; found C 32.01, H 7.25, N 5.31. FT-IR (KBr): $\tilde{\nu}$ = 3428 (br), 2963 (w), 2923 (w), 1568 (s), 1414 (m), 1261 (m), 1095 (w), 1025 (w), 803 (m), 678 (w), 560 (w), 516 (m), 465 (m) cm^{-1}. TGA: 50–121 °C (14.99% weight loss), 121–167 °C (7.41% weight loss), 167–264 °C (47.53% weight loss), 264–456 °C (residue 24.73%).

Synthesis of Cu$_3$(dmae)$_3$(acac)$_2$Cl (2): 1.25 g (1.67 mmol) of [Cu(dmae)Cl]$_4$ in 20 mL of toluene were transferred to 0.50 g (4.44 mmol) of Na(acac) which was prepared by reaction of an appropriate amount of Na metal with acetylacetonate in toluene at room temperature. The mixture was stirred for 3 h and filtered

Table 2. Crystal data and structure refinement for compounds **1**, **2** and **3**.

Empirical formula	$C_{14}H_{38}Cu_2N_2O_{10}$	$C_{22}H_{44}ClCu_3N_3O_7$	$C_{24}H_{40}Cu_4F_{12}N_4O_{12}$
Formula weight	521.54	688.67	1058.80
Solvent	toluene	toluene	toluene/THF
Crystal habit, color	plate, blue	block, pale turquoise	block, blue
Temperature [K]	100(2)	150(2)	100(2)
Crystal system	triclinic	triclinic	monoclinic
Space group	$P\bar{1}$	$P\bar{1}$	$P2_1/c$
a [Å]	6.3586(9)	8.4980(1)	13.8517(17)
b [Å]	8.2571(12)	12.6650(2)	20.726(3)
c [Å]	10.9032(15)	14.7460(2)	14.0355(17)
α [°]	79.903(2)	80.413(1)	90
β [°]	81.783(2)	83.638(1)	104.249(2)
γ [°]	77.114(2)	75.514(1)	90
Volume [Å^3]	546.17(13)	1511.18(4)	3905 (8)
Z	1	2	4
Density (calculated) [Mg/m^3]	1.586	1.513	1.801
Absorption coefficient [mm^{-1}]	1.997	2.221	2.264
F(000)	274	714	2128
Crystal size [mm]	0.37 × 0.34 × 0.09	0.30 × 0.20 × 0.20	0.60 × 0.50 × 0.30
θ range for data collection [°]	1.91 to 28.28	3.54 to 27.57	1.52 to 28.28
Index ranges	$-8 \le h \le 8$	$-11 \le h \le 11$	$-18 \le h \le 18$
	$-10 \le k \le 11$	$-16 \le k \le 16$	$-27 \le k \le 27$
	$-14 \le l \le 14$	$-19 \le l \le 19$	$-18 \le l \le 18$
Reflections collected	5717	31164	39593
Independent reflections	2709 [R(int) = 0.0165]	6875 [R(int) = 0.0406]	9695 [R(int) = 0.0383]
Absorption correction	multiscan	semiempirical from equivalents	multiscan
max. / min. transmission	0.835 / 0.635	0.28 / 0.24	0.507 / 0.356
Data / restraints / parameters	2709 / 4 / 149	6875 / 0 / 336	9695 / 46 / 543
Goodness-of-fit on F^2	1.081	1.051	1.080
Final R indices [$I>2\sigma(I)$]	R_1 = 0.0251, $wR2$ = 0.0659	R_1 = 0.0250, $wR2$ = 0.0632	R_1 = 0.0446, $wR2$ = 0.1193
R indices (all data)	R_1 = 0.0264, $wR2$ = 0.0670	R_1 = 0.0277, $wR2$ = 0.0645	R_1 = 0.0520, $wR2$ = 0.1234
Largest diff. peak and hole[e Å^{-3}]	0.574 and –0.659	0.922 and –0.442	1.278 and –0.779

through cannula to remove the NaCl produced. The filtrate was evaporated to dryness under vacuum and the solid was redissolved in 5 mL of toluene and stored at –10 °C for one week to give blue crystals suitable for X-ray diffraction; yield 79%, m.p. 138 °C. $C_{22}H_{44}ClCu_3N_3O_7$ (688.67): calcd. C 38.37, H 6.44, N 6.10; found C 37.98, H 6.29, N 5.63. FT-IR (KBr): $\tilde{\nu}$ = 2964 (m), 2896 (w), 1579 (s), 1551 (m), 1528 (s), 1461 (s), 1413 (w), 1389 (w), 1277 (m), 1261 (m), 1184 (w), 1071 (s), 1021 (s), 952 (s), 900 (m), 785 (s), 650 (m), 614 (m), 513 (m), 455 (s) cm^{-1}. TGA: 71–255 °C (21.55% weight loss); 255–276 °C (39.52% weight loss); 276–350 °C (residue 25.99%).

Synthesis of [Cu(dmae)(TFA)]$_4$ (3): 0.71 g (7.96 mmol) of dmaeH and 1.07 g (7.96 mmol) of trifluoroacetic acid (TFAH) were added to a suspension of 1.0 g (7.96 mmol) of $Cu(OCH_3)_2$ [which was synthesized by the reaction of an appropriate amount of $CuCl_2$ (anhydrous) with CH_3OLi in dry methanol] in 20 mL of THF. The reaction mixture was stirred for 2 h at room temperature, evaporated to dryness under vacuum and then the solid was redissolved in 10 mL of THF to give blue crystals suitable for X-ray diffraction; yield 80%, m.p. 210 °C. $C_{24}H_{40}Cu_4F_{12}N_4O_{12}$ (1058.80): calcd. C 27.23, H 3.80, N 5.29; found C 27.93, H 3.88, N 5.62. FT-IR (KBr): $\tilde{\nu}$ = 2982 (m), 2923 (w), 2884 (m), 1692 (s), 1593 (m), 1466 (w), 1420 (m), 1276 (w), 1210 (m), 1202 (s), 1135 (s), 1120 (m), 1065 (s), 1016 (m), 952 (s), 901 (m), 839 (m), 795 (s), 726 (s), 637 (m), 525 (m), 432 (w) cm^{-1}. TGA: 175–300 °C (residue 27.76%).

Deposition of Thin Films: Copper thin films were deposited on a soda glass substrate in a hot-walled reactor by gas-phase reactions of the precursors in an argon environment at atmospheric pressure using a self-designed Aerosol-Assisted Chemical Vapor Deposition assembly described elsewhere.[36] The substrates of dimensions 1.5 × 3 cm were degreased by successive treatment with acetone and water and positioned horizontally in a glass tube in a furnace fitted with an aerosol generator. The argon carrier gas flow rate was adjusted at 25 cm^3/min and the precursor solution (0.3 g/25 mL) was injected at a rate of 0.2 mL/min. Optimum parameters for the growth of thin films are listed in Table 3.

Table 3. Growth conditions for the deposition of copper thin film by AACVD.

Parameters	Values
Precursor concentration	0.3 g/25 mL (toluene)
Carrier gas (Ar) flow rate [cm^3/min]	25
Sample solution injection [mL/min]	0.2
Substrate	soda glass
Deposition time	125 min
Deposition temperature	450 °C for **1** 350 °C for **2** 300 °C for **3**

Acknowledgments

M. S., A. A. T., M. H., and M. M. would like to thank the Higher Education Commission Islamabad, Pakistan for financial support through the "Indigenous 5000 and open merit 200 Ph. D. Scholarship Scheme" and Pakistan Science foundation [PSF/RES/C-QU/CHEM(408)]. The X-ray diffractometer at Youngstown State University was funded by NSF Grant 0087210, Ohio Board of Regents Grant CAP-491, and by Youngstown State University.

[1] a) P. Braunstein, L. A. Oro, P. R. Raithby, *Metal Clusters in Chemistry*, Eds.; Wiley-VCH, Weinheim, Germany, **1999**, vols. 1–3; b) R. E. P. Winpenny, *J. Chem. Soc., Dalton Trans.* **2002**, 1–10; R. E. P. Winpenny, *Adv. Inorg. Chem.* **2001**, *52*, 1.
[2] a) D. Gatteschi, R. Sessoli, A. Cornia, *Chem. Commun.* **2000**, 725–732; b) D. Gatteschi, R. Sessoli, *Angew. Chem. Int. Ed.* **2003**, *42*, 268–297.
[3] J. S. Miller, D. A. Dougherty, *Mol. Cryst. Liq. Cryst.* **1989**, 176.
[4] J. S. Miller, M. Drillon, *Magnetism: Molecules to Materials*, Wiley-VCH, Weinheim, Germany, **2001**–**2002**, vol. 1–4.
[5] D. Gatteschi, L. Pardi, A. L. Barra, A. Müller, J. Döring, *Nature* **1991**, *354*, 463–465.
[6] C. Delfs, D. Gatteschi, L. Pardi, R. Sessoli, K. Wieghardt, D. Hanke, *Inorg. Chem.* **1993**, *32*, 3099–3103.
[7] a) R. Sessoli, D. Gatteschi, A. Caneschi, M. A. Novak, *Nature* **1993**, *365*, 141–143; b) S. M. J. Aubin, N. R. Dilley, M. Wemple, M. B. Maple, G. Christou, D. N. Hendrickson, *J. Am. Chem. Soc.* **1998**, *120*, 839–840; c) A. Cornia, D. Gatteschi, R. Sessoli, *Coord. Chem. Rev.* **2001**, *219*, 573–604.
[8] I. G. Dance, in: *Comprehensive Coordination Chemistry* (Eds.: G. Wilkinson, R. D. Gillard, J. A. McCleverty), Pergamon, Oxford, U. K., **1987**, vol. 1, pp. 135.
[9] A. Muller, F. Peters, M. T. Pope, D. Gatteschi, *Chem. Rev.* **1998**, *98*, 239–271.
[10] a) M. Hamid, A. A. Tahir, M. Mazhar, F. Ahmad, K. C. Molloy, G. Kociok-Kohn, *Inorg. Chim. Acta* **2008**, *361*, 188–194; b) M. Hamid, A. A. Tahir, M. Mazhar, M. Zeller, K. C. Molloy, A. D. Hunter, *Inorg. Chem.* **2006**, *45*, 10457–10466.
[11] S. Wang, *J. Cluster Sci.* **1995**, *6*, 463–484.
[12] a) D. C. Bradley, *Chem. Rev.* **1989**, *89*, 1317–1322; b) O. Poncelet, L. G. Hubert-Pfalzgraf, J. C. Daran, R. J. Astier, *J. Chem. Soc., Chem. Commun.* **1989**, 1846–1848; c) K. G. Caulton, L. G. Hubert-Pfalzgraf, *Chem. Rev.* **1990**, *90*, 969–995; d) O. Poncelet, W. J. Sartain, L. G. Hubert-Pfalzgraf, K. Folting, K. G. Caulton, *Inorg. Chem.* **1989**, *28*, 263–267; e) S. C. Goel, M. Y. Chiang, W. E. Buhro, *Inorg. Chem.* **1990**, *29*, 4640–4646.
[13] M. F. Yan, *Ceramic Superconductors*, American Ceramic Society, Westerville, OH, **1988**.
[14] a) P. Doppelt, *Microelectron. Eng.* **1997**, *38*, 89–95; b) V. N. Vertoprakhov, S. A. Krupoder, *Russ. Chem. Rev.* **2000**, *69*, 1057–1082.
[15] Y. Chi, P.-F. Hsu, C.-S. Liu, W.-L. Ching, T.-Y. Chou, A. J. Carty, S.-M. Peng, G.-H. Lee, S.-H. Chuang, *J. Mater. Chem.* **2002**, *12*, 3541–3550.
[16] a) N. Awaya, K. Ohno, Y. Arita, *J. Electrochem. Soc.* **1995**, *142*, 3173–3179; b) Y. D. Chen, A. Reisman, I. Turlik, D. Temple, *J. Electrochem. Soc.* **1995**, *142*, 3903–3911.
[17] a) H. Choi, S. Hwang, *Chem. Mater.* **1998**, *10*, 2326–2328; b) A. Devi, J. Goswami, R. Lakshmi, S. A. Shivashankar, S. Chandrasekwran, *J. Mater. Res.* **1998**, *13*, 687–692.
[18] H. S. Horowitz, S. J. McLain, A. W. Sleight, J. D. Druliner, P. L. Gai, M. J. VanKavelaar, J. L. Wagner, B. D. Biggs, S. J. Poon, *Science* **1989**, *243*, 66–69.
[19] S. C. Goel, K. S. Kramer, M. Y. Chiang, W. E. Buhro, *Polyhedron* **1990**, *9*, 611–613.
[20] a) J. Hambrock, R. Becker, A. Birkner, J. Weiß, R. A. Fischer, *Chem. Commun.* **2002**, 68–69; b) R. Becker, A. Devi, J. Weiß, U. Weckenmann, M. Winter, C. Kiener, H.-W. Becker, R. A. Fischer, *Chem. Vap. Deposition* **2003**, *9*, 149–156.
[21] E. Lay, Y.-H. Song, Y.-C. Chiu, Y.-M. Lin, Y. Chi, A. J. Carty, S.-M. Peng, G.-H. Lee, *Inorg. Chem.* **2005**, *44*, 7226–7233.
[22] a) V. M. Donnelly, M. E. Gross, *J. Vac. Sci. Technol. A* **1993**, *11*, 66–77; b) P.-F. Hsu, Y. Chi, T.-W. Lin, C.-S. Liu, A. J. Carty, S.-M. Peng, *Chem. Vap. Deposition* **2001**, *7*, 28–31.
[23] H. K. Shin, K.-M. Chi, M. J. Hampden-Smith, T. T. Kodas, J. D. Farr, M. F. Paffett, *Mat. Res. Soc. Symp. Proc.* **1990**, *204*, 421.
[24] a) V. L. Young, D. F. Cox, M. E. Davis, *Chem. Mater.* **1993**, *5*, 1701–1709; b) P. Doppelt, *Coord. Chem. Rev.* **1998**, *178–180*, 1785–1809.
[25] a) J. A. T. Norman, D. A. Robert, A. K. Hochberg, P. Smith, J. E. Peterson, J. E. Parmeter, C. A. Apblett, T. R. Omstead,

Thin Solid Films **1995**, *262*, 46–51; b) Y.-M. Park, J.-H. Son, S.-W. Kang, S. W. Rhee, *J. Mater. Res.* **1999**, *14*, 975–979.
[26] M. Hamid, A. A. Tahir, M. Mazhar, M. Zeller, K. C. Molloy, A. D. Hunter, *Inorg. Chem.* **2006**, *45*, 10457–10466.
[27] J. Zhang, L. G. Hubert-Pfalzgraf, D. Luneau, *Inorg. Chem. Commun.* **2004**, *7*, 979–984.
[28] J.-C. Zheng, R. J. Rousseau, S. Wang, *Inorg. Chem.* **1992**, *31*, 106–110.
[29] a) ICDD powder diffraction database file card number [03-065-9026]; b) I. Suh, H.-K. Ohta, Y. Wase, *J. Mater. Sci.* **1988**, *23*, 757–760.
[30] Bruker Advanced X-ray Solutions SAINT (Version 6.45), Bruker AXS Inc., Madison, Wisconsin, USA, **1997**–**2003**.
[31] a) Bruker Advanced X-ray Solutions SMART for WNT/**2000** (Version 5.628), Bruker AXS Inc., Madison, Wisconsin, USA, **1997–2002**; b) Bruker Advanced X-ray Solutions *SHELXTL* (Version 6.10), Bruker AXS Inc., Madison, Wisconsin, USA, **2000**.
[32] Z. Otwinowski, W. Minor, *Methods in Enzymology* (Eds.: C. W. Carter Jr., R. M. Sweet), Academic Press, New York, **1997**, vol. 276, pp. 307–326.
[33] R. H. Blessing, *Acta Crystallogr., Sect. A* **1995**, *51*, 33–38.
[34] SIR 97 A. Altomare, M. C. Burla, M. Camalli, G. L. Cascarano, C. Giacovazzo, A. Guagliardi, A. G. G. Moliterni, G. Polidori, R. Spagna, *J. Appl. Crystallogr.* **1999**, *32*, 115–119.
[35] *SHELXL97 – Program for Crystal Structure Analysis (Release 97–2)*, G. M. Sheldrick, Institut für Anorganische Chemie der Universität, Tammannstrasse 4, Göttingen, Germany, **1998**.
[36] A. A. Tahir, K. C. Molloy, M. Mazhar, G. Kociok-Köhn, M. Hamid, S. Dastgir, *Inorg. Chem.* **2005**, *44*, 9207–9212.

Received: October 27, 2008
Published Online: February 5, 2009

